The Borosulfate Story Goes on—From Alkali and Oxonium Salts to Polyacids

Michael Daub,[a] Karolina Kazmierczak,[b] Henning A. Höppe,*[b] and Harald Hillebrecht*[a]

Abstract: The structural principles of borosulfates derived from the B/S ratio are confirmed and extended to new representatives of this class showing novel motifs. According to the composition, $Na[B(S_2O_7)_2]$ ($P2_1/c$; $a=$ 10.949(6), $b=8.491(14)$, $c=$ 12.701(8) Å; $\beta=110.227(1)°$; $Z=4$) and $K[B(S_2O_7)_2]$ (Cc; $a=11.3368(6)$, $b=$ 14.662(14), $c=13.6650(8)$ Å; $\beta=$ 94.235(1)°; $Z=8$) contain isolated $[B(S_2O_7)_2]^-$ ions, in which the central BO_4 tetrahedron is coordinated by two disulfate units. The alkali cations have coordination numbers of 7 (Na) and 8 (K), respectively. The structure of $Cs[B(S_2O_7)(SO_4)]$ ($P2_1/c$; $a=$ 10.4525(6), $b=11.3191(14)$, $c=$ 8.2760(8) Å; $\beta=103.206(1)$; $Z=4$) combines, for the first time, sulfate and disulfate units into a chain structure. Cs has a coordination number of 12. The same structural units were found in $H[B(S_2O_7)(SO_4)]$ ($P2_1/c$; $a=$ 15.6974(6), $b=11.4362(14)$, $c=$ 8.5557(8) Å; $\beta=90.334(3)°$; $Z=8$). This compound represents the first example of a polyacid. The hydrogen atoms were located and connect the chains to form layers through hydrogen-bonding bridges. $H_3O[B(SO_4)_2]$ ($P4/ncc$; $a=$ 9.1377(6), $c=7.3423(8)$ Å; $Z=4$) is the first oxonium compound of this type to be found. The BO_4 tetrahedra are linked by SO_4 tetrahedra to form linear chains similar to those in SiS_2. The chains form a tetragonal rod packing structure with H_3O^+ between the rods. The structures of borosulfates can be classified following the concept described by Liebau for silicates, which was extended to borophosphates by Kniep et al. In contrast to these structures, borosulfates do not comprise B-O-B bonds but instead contain S-O-S connections. All compounds were obtained as colourless, moisture-sensitive single crystals by reaction of B_2O_3 and the appropriate alkali salt in oleum.

Introduction

Very recently, $K_5[B(SO_4)_4]$ was characterised as the first representative of the borosulfates. The prominent structural feature is a supertetrahedral anion with a central BO_4 tetrahedron surrounded by four SO_4 tetrahedra.[1] With a ratio of 1:4 between BO_4 and SO_4 tetrahedra, the supertetrahedral units are not condensed, leading to a charge of −5. Later on, the same unit was found in the two polymorphs of $Na_5[B(SO_4)_4]$.[2] In compounds with a B/S ratio of 1:3, the supertetrahedral units are condensed into linear chains; representative compounds with this structure are $K_3[B(SO_4)_3]$ and $Rb_3[B(SO_4)_3]$.[2] Further condensation into a three-dimensional network was found for $Li[B(SO_4)_2]$,[2] with a B/S ratio of 1:2. This series shows the similarity to the structural chemistry of silicates as the same relationships were found for the Si/O ratio, that is, non-condensed units in orthosilicates with SiO_4^{4-} (for example, $Zr[SiO_4]$), chains with $[SiO_3^{2-}]_n$ (pyroxenes like orthoenstatite, $Mg_2[Si_2O_6]$) and a 3D network for the modifications of SiO_2.

Borosulfate structures are based on alternating BO_4 and SO_4 tetrahedra connected by common apices, that is, BO_4 with SO_4 and vice versa. Modifying this pattern, $Li[B(S_2O_7)_2]$ shows the possibility of various structures.[2] Here, the central BO_4 tetrahedron is coordinated by two disulfate units. The B/S ratio of 1:4 still leads to a non-condensed tetrahedral moiety with a reduced charge due to the condensation of the terminal sulphate anions. This feature was recently described by Wickleder et al. for complexes of transition metals like $[Au(S_2O_7)_2]^-$[3] and $[Pd(S_2O_7)_2]^{2-}$,[4] and for sulfates of Group 14 elements (Si, Ge).[5] This shows the astonishing versatility of complex sulfates.

The key to accessing new borosulfates is an the appropriate design of the experimental conditions. Borosulfates may, in principle, be obtained by several different routes. As well as simple stoichiometric solid-state syntheses, for example, $ABO_2+2A_2S_2O_7\rightarrow A_5B(SO_4)_4$, or precipitation from more or less concentrated sulfuric acid, there are a great number of promising thermal decomposition reactions, like the loss of H_2O and/or SO_3 from H_2SO_4, H_3BO_3, $AHSO_4$, A_2SO_4, and so forth, which result in the formation of borosulfates. Be-

[a] Dipl.-Chem. M. Daub, Prof. Dr. H. Hillebrecht
Institut für Anorganische und Analytische Chemie
Albert-Ludwigs-Universität Freiburg
Albertstrasse 21, 79104 Freiburg (Germany)
E-mail: harald.hillebrecht@ac.uni-freiburg.de

[b] Dr. K. Kazmierczak, Prof. Dr. H. A. Höppe
Institut für Physik, Universität Augsburg
Universitätsstrasse 1, 86159 Augsburg (Germany)
E-mail: henning@ak-hoeppe.de

cause there are so many different reaction pathways, the chemical behaviour is very complex, leading to an unclear situation. In addition, borosulfates are very sensitive to moisture so the isolation and characterisation of single crystals is not trivial and some compounds may require the presence of a mother liquor or cannot be separated from the solvent without decomposition. Furthermore, the synthesis of single-phase samples can be problematic because of the changing conditions during the reaction. Both of these aspects can hinder the application of methods for the characterisation of these compounds, for example, NMR spectroscopy, X-ray powder diffraction, or vibrational spectroscopy, and structural characterisation.

Herein, we report the synthesis of new borosulfates with a focus on the use of oleum as the reactive solvent. We show that the existence of disulfate complexes can be extended to other monovalent cations. Furthermore, we shall demonstrate that sulfate and disulfate units can coexist in the same compound. Finally, we have observed structural principles that are unknown for silicates. The focus of this contribution is structural characterisation based on single-crystal data and the classification of the structures with respect to similar borophosphates.

Results and Discussion

Na[B(S$_2$O$_7$)$_2$] and K[B(S$_2$O$_7$)$_2$]: Both compounds are examples of borosulfates with a B/S ratio of 1:4. According to the principles of borosulfates, non-condensed units are expected.

Na[B(S$_2$O$_7$)$_2$]: As indicated by the composition, the structure of Na[B(S$_2$O$_7$)$_2$] represents the same principle as was found for the analogous Li compound. Figure 1 shows the unit cell, which contains one symmetry independent unit. The central BO$_4$ tetrahedron is coordinated by two disulfate anions. The result is a pseudo-tetrahedral monovalent anion
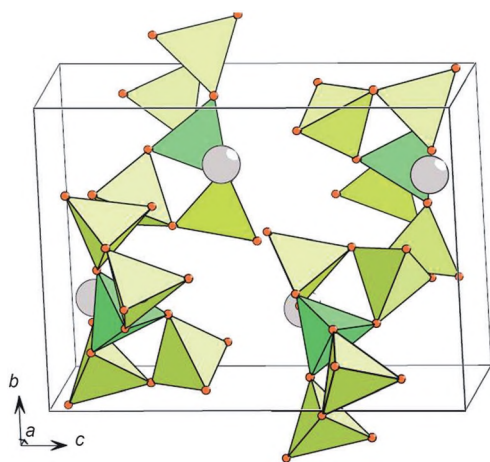

Figure 1. Crystal structure of Na[B(S$_2$O$_7$)$_2$] (green: BO$_4$ tetrahedra, yellow: SO$_4$ tetrahedra, grey spheres: Na).

[B(S$_2$O$_7$)$_2$]$^-$. Each of these units is surrounded by other units in a two-fold capped trigonal prismatic manner, with the shortest distances in the [010] direction.

The variation of B−O and S−O distances follows crystallographic expectations. B−O distances range between 1.460 and 1.489 Å, and O-B-O angles range between 105.8 and 112.9° (see Figure 2). For the S$_2$O$_7^{2-}$ moiety, the shortest
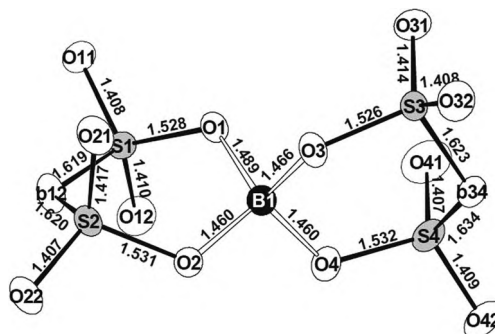

Figure 2. The [B(S$_2$O$_7$)$_2$]$^-$ ion in Na[B(S$_2$O$_7$)$_2$], in which the ellipsoids represent 65% probability.

S−O distances are those to the terminal oxygen atoms, intermediate values are observed for oxygen atoms connected to the BO$_4$ tetrahedron and the longest distances are found between the SO$_4$ tetrahedra. Enlarged angles (with respect to those expected within tetrahedra) of around 120° are detected between the terminal oxygen atoms, and smaller angles were found between the bridging atoms (100–102°). The B-O-S and S-O-S angles are also situated around 120°, in agreement with findings for other borosulfates[1,2] and disulfates (for example, K$_2$S$_2$O$_7$[6]).

According to a 5+2 pattern, only terminal oxygen atoms surround sodium (Figure 3). All terminal oxygen atoms participate in this coordination except O41. This explains the enlarged displacement parameter for O41 because it is not involved in an interaction with Na$^+$. Additionally, it can be regarded as an indirect indicator of the quality of the single-
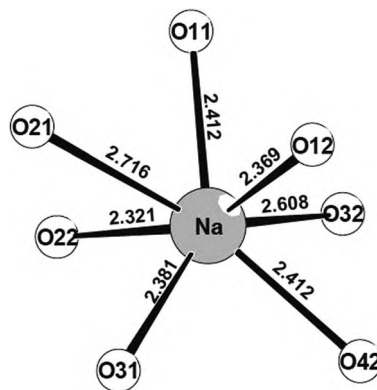

Figure 3. Coordination of the sodium atoms in Na[B(S$_2$O$_7$)$_2$], with distances up to 3.2 Å considered.

crystal data. Similar observations were made for Li[B-(S_2O_7)_2]. Since Li$^+$ is smaller than Na$^+$, its coordination number is reduced to six. Two of the terminal oxygen atoms do not coordinate Li$^+$ and consequently show enlarged displacement parameters.[2]

K[B(S_2O_7)_2]: The crystal structure of K[B(S_2O_7)_2] (Figure 4) complements the findings for the similar sodium and lithium compounds. Again, the BO_4 tetrahedron is surrounded by two disulfate units. K$^+$ and [B(S_2O_7)_2]$^-$ are arranged in a CsCl-like manner, which explains the pseudo-cubic metric.

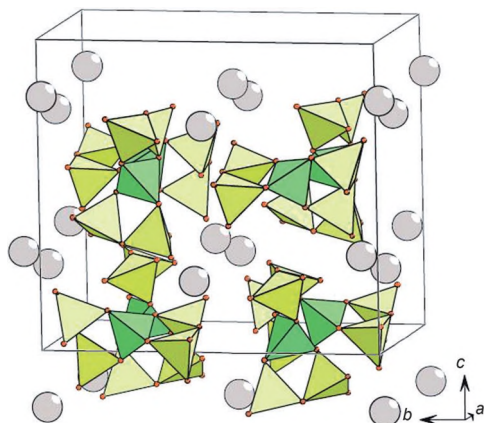Figure 4. Crystal structure of K[B(S_2O_7)_2] (green: BO_4 tetrahedra, yellow: SO_4 tetrahedra, grey spheres: K).

The unit cell contains two independent [B(S_2O_7)_2]$^-$ ions with very similar geometries. One of these units is shown in Figure 5. Distances and angles are in line with the previous results, that is, B−O distances range between 1.453 and
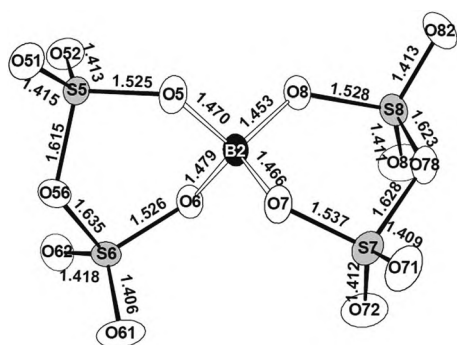

Figure 5. The [B(S_2O_7)_2]$^-$ ion in K[B(S_2O_7)_2], in which distances are given in Å and ellipsoids represent 65% probability.

1.479 Å, there are relatively shorter terminal S−O distances (1.406–1.418 Å), which are intermediate for bridging S−O bonds to BO_4 tetrahedra (1.525–1.537 Å) and longer ones for the bridging S−O bonds within the S_2O_7^{2-} ion (1.615–1.635 Å). The variation in bonding angles is very similar to Na[B(S_2O_7)_2] and therefore we will not discuss these in detail.

According to the larger radius of K$^+$, the coordination number increases to eight (Figure 6). In contrast to the lithium and sodium compounds, every terminal oxygen atom contributes to the cation's coordination sphere.
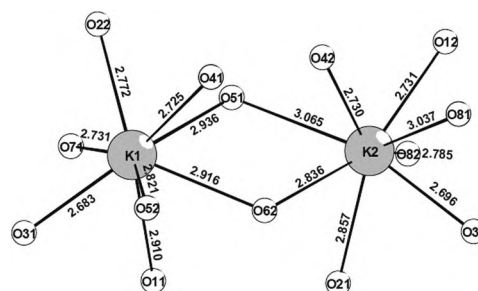
Figure 6. Coordination of the potassium atoms in K[B(S_2O_7)_2], with distances up to 3.4 Å considered.

Cs[B(SO_4)(S_2O_7)]: Cs[B(SO_4)(S_2O_7)] represents the first caesium borosulfate. Furthermore, it is the first example in which sulfate and disulfate units are present in the same moiety. According to the B/S ratio of 1:3, a chain structure is expected; this pattern holds for Cs[B(SO_4)(S_2O_7)]. However, in contrast to the open-branched vierer single chains found in K_3[B(SO_4)_3)] and Rb_3[B(SO_4)_3)],[2] the two terminal SO_4 units are substituted by disulfate units. Thus, a cyclo-branched vierer single chain is formed and the charge of the repeating unit is reduced from −3 to −1. Figure 7 shows the unit cell of Cs[B(SO_4)(S_2O_7)]. The chains run along the *c* axis and form a tetragonal rod packing structure with the Cs$^+$ ions between them.

The observed distances and angles within the anionic chain [B(SO_4)(S_2O_7)_2]$^-$ lie perfectly between the bridging sulfate units in A_3[B(SO_4)_3)] (A = K, Rb), Li[B(SO_4)_2], and H_3O[B(SO_4)_2] (see below), and the bridging disulfate units
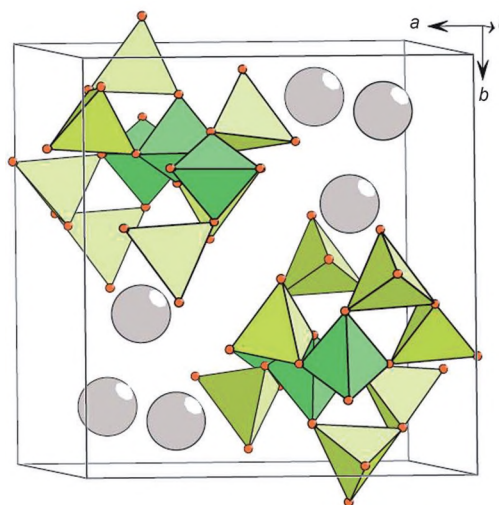
Figure 7. Crystal structure of Cs[B(SO_4)(S_2O_7)] (green: BO_4 tetrahedra, yellow: SO_4 tetrahedra, grey spheres: Cs)
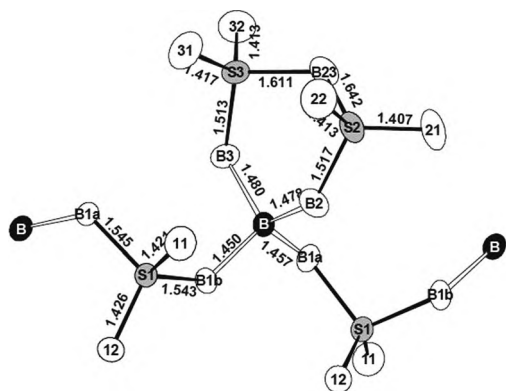
Figure 8. The repeating unit $[B(SO_4)(S_2O_7)_2]^-$ of the chain anion in Cs[B-$(SO_4)(S_2O_7)_2]$, in which distances are given in Å and ellipsoids represent 65% probability.

in $A[B(S_2O_7)_2]$ (A = Li, Na, K) (Figure 8). Between the two structural elements there are small but significant differences. The B−O bonds to the SO_4 group (1.450–1.457 Å) are slightly shorter than those to the S_2O_7 anion (1.478–1.480 Å). On the other hand, the terminal S−O^{term} bonds of the SO_4 anion (1.421–1.426 Å) and the bridging S−O^{br} bonds (1.545 Å) to the tetrahedron are longer than the corresponding distances in the S_2O_7 group (1.407–1.417 and 1.513–1.517 Å). Again, the longest distances remain the bridging S−O^{br} bonds of the disulfate unit (1.611–1.642 Å). Enlarged angles of around 120° are observed between the terminal O atoms (O^{term}-S-O^{term}) and for the bridging oxygen atoms (S-O^{br}-S). The largest angles were found for the bridges between the BO_4 and SO_4 tetrahedra (B-O^{br}-S: 126–131°).

The Cs$^+$ ions are placed between the chains. Their coordination number of 12 (Figure 9) is in line with the increased radius of caesium ions.
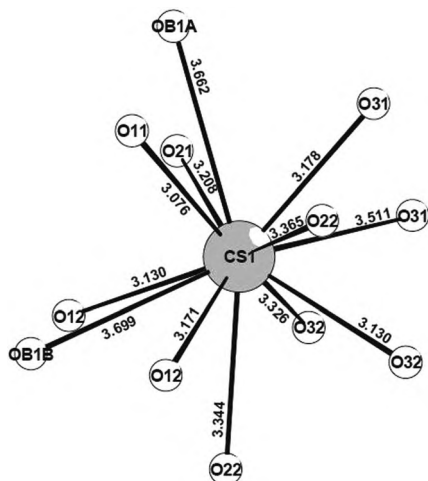

Figure 9. Coordination of the caesium ions in Cs[B(SO_4)(S_2O_7)], with distances up to 4.5 Å considered.

H[B(SO_4)(S_2O_7)]: The crystal structure of H[B(SO_4)(S_2O_7)] is similar to that of the Cs compound. The B/S ratio of 1:3

points towards a chain structure. According to the composition H[B(SO_4)(S_2O_7)], the connectivity pattern is the same as in Cs[B(SO_4)(S_2O_7)], that is, the BO_4 tetrahedra are linked by SO_4 tetrahedra in a single vierer chain and the two remaining oxygen atoms are bound to a disulfate unit. There are two independent chains running along the c axis (Figure 10).
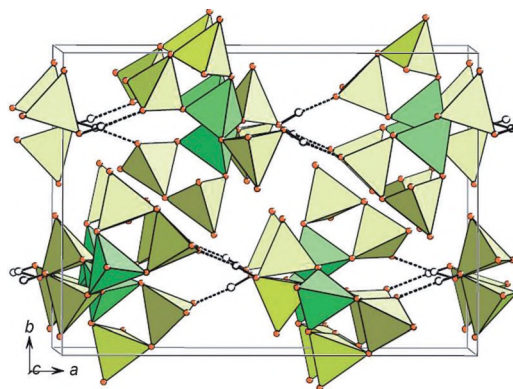
Figure 10. Crystal structure of H[B(SO_4)(S_2O_7)] (green: BO_4 tetrahedra, yellow: SO_4 tetrahedra, white spheres: H, dotted lines: hydrogen bonds).

In contrast to Cs[B(SO_4)(S_2O_7)], hydrogen bonds in H[B-(SO_4)(S_2O_7)] connect the borosulfate chains into layers perpendicular to the b axis. The difference between the two chains is the deviation in the orientation of the tetrahedra directly involved in hydrogen-bonding bridges. Both hydrogen positions were unequivocally located by a difference Fourier synthesis at the final stage of the refinement. They appeared as the significantly highest residual electron densities. Each of the two different hydrogen atoms is bound to one of the terminal oxygen atoms of the sulfate ion. In both cases, the hydrogen bonds point towards a terminal oxygen atom of the disulfate group. The strength of these bonds is, however, different. The O−O distance within the group OH1−H1···O51 is 2.672 Å, which corresponds to a medium-strength hydrogen bond.[7] For the group OH2−H2···O21, this distance amounts to 2.494 Å, which fits with a strong hydrogen-bonding bridge.

The formation of hydrogen bonds influences the geometry of the chain (Figure 11). The differences become clear by comparing the structure with the chain found in Cs[B(SO_4)-(S_2O_7)]. Most evident is the elongation of the terminal S−O^{term} bond of the isolated SO_4 tetrahedron by the addition of a proton. The relatively shorter distances to O11 and O41 are 1.401 and 1.404 Å, respectively, whereas the longer distances to OH1 (1.511 Å) and OH2 (1.493 Å) are comparable to those of the S−O bonds connected to the BO_4 tetrahedron (1.48–1.51 Å). Small changes are also caused in the disulfate group, for which one out of the four terminal oxygen atoms participates in the hydrogen bridge (O21 and O51, respectively). Consequently, the S−O distances are enlarged from 1.405–1.410 Å to 1.420/1.426 Å. Furthermore,

16957

Figure 11. The repeating unit $[B(SO_4)(S_2O_7)_2]^-$ of the two different chain anions in $H[B(SO_4)(S_2O_7)_2]$, with distances given in Å.

the asymmetry of the bridging S–O^{br} bond within the disulfate unit is more pronounced (1.606/1.645 Å).

The structural and chemical similarity between $H[B(SO_4)(S_2O_7)]$ and $Cs[B(SO_4)(S_2O_7)]$ requires a comparison. Formally, $H[B(SO_4)(S_2O_7)]$ represents a two-fold superstructure of $Cs[B(SO_4)(S_2O_7)]$ obtained by doubling the c axis. Figure 12 shows projections of these structures on the a–c plane. The b and c axes (chain direction) remain nearly unchanged ($b = 11.44/11.32$ Å; $c = 8.56/8.28$ Å) for these two compounds. However, the formal substitution of Cs$^+$ by H$^+$ leads to a significant shrinkage along the a axis. Thus, the doubling of the a axis of the caesium compound ($a = 10.45$ (2×)) yields $a_H = 15.70$ Å. On first sight, these values do not seem to fit, but the increase in the unit-cell volume is in accord with the larger ionic volume of Cs$^+$, and the larger lattice parameter b also coincides with the radius of Cs$^+$. Despite a similar arrangement, the rotation of the tetrahedra causes the difference and accordingly the doubling of the unit cell. The relationship between the structures is reflected in the X-ray diffraction intensities of $H[B(SO_4)(S_2O_7)]$.[8]

The H atom was unequivocally located near one of the terminal oxygen atoms of the SO$_4$ tetrahedron. It is part of a hydrogen-bonding system that is very similar to that found

Figure 12. Crystal structures of $Cs[B(SO_4)(S_2O_7)]$ (top) and $H[B(SO_4)(S_2O_7)]$ (bottom), with projection in the [010] direction (green: BO$_4$ tetrahedra, yellow: SO$_4$ tetrahedra, grey: Cs, black: H).

in H_2SO_4 and $H_2S_2O_7$. In H_2SO_4,[9] the S–O distances in the tetrahedron split to 1.426 and 1.537 Å. The distance between oxygen atoms within a hydrogen-bonding bridge is 2.648 Å. In $H_2S_2O_7$,[10] the S–O bond length splitting amounts to 1.41 and 1.52 Å, and the O···O distance is 2.62 Å. Because no other cation is present, we classify $H[B(SO_4)(S_2O_7)]$ as a one-dimensional hetero-polysulfuric acid.

$H_3O[B(SO_4)_2]$: $H_3O[B(SO_4)_2]$ represents a borosulfate with oxonium ions (H$_3$O$^+$) as the cations. The crystal structure is shown in Figure 13. Again, the BO$_4$ tetrahedra are surround-

Figure 13. Crystal structure of $H_3O[B(SO_4)_2]$, with projection in the [001] direction (green: BO$_4$ tetrahedra, yellow: SO$_4$ tetrahedra, red spheres: O, white spheres: H).

ed by four SO$_4$ tetrahedra. According to the B/S ratio of 1:2, each SO$_4$ tetrahedron is connected to two BO$_4$ tetrahedra but in contrast to Li[B(SO$_4$)$_2$], which has the same ratio, a linear chain is formed. The "supertetrahedra" share a common edge instead of corners (as in the Li compound). Alternatively, the crystal structure of H$_3$O[B(SO$_4$)$_2$] can be described as a tetragonal rod structure[11] of [B(SO$_4$)$_2$]$^-$ chains with disordered H$_3$O$^+$ cations between them.

According to the space-group symmetry, the chains feature perfect D_{2d} symmetry. Figure 14 shows the repeating unit. The distances are in the typical range expected for borosulfates, a B$-$O distance of 1.469 Å, short S$-$O^{term} distances (1.415 Å) and longer S$-$O^{br} distances (1.530 Å).
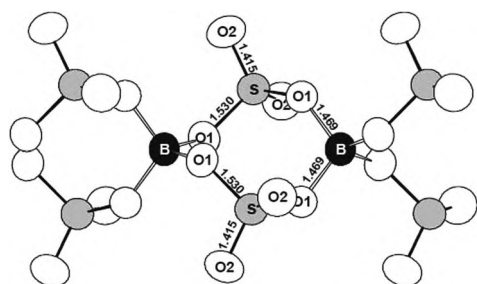

Figure 14. The repeating unit [B(SO$_4$)$_2$]$^-$ in H$_3$O[B(SO$_4$)$_2$], in which distances are given in Å and ellipsoids represent 65% probability.

The H$_3$O$^+$ cations are located between the chains (Figure 15). The position of the hydrogen atom was located by difference Fourier synthesis; its consideration improved the R values significantly (formerly: $R_1 = 0.039$, $wR_2 = 0.091$;
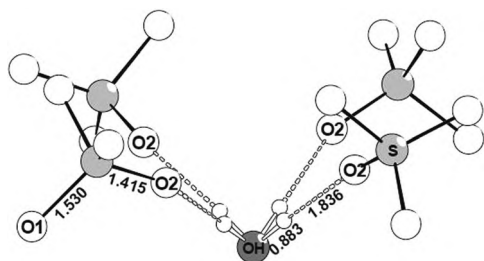

Figure 15. Coordination of H$_3$O$^+$ in H$_3$O[B(SO$_4$)$_2$], with distances given in Å.

finally: $R_1 = 0.030$, $wR_2 = 0.068$,). The hydrogen atom was refined with restrictions. The use of a free-site occupation factor with a fixed displacement parameter revealed a value of 72(4)%. According to the site symmetry $\bar{4}$ of the O atom, the positions of the hydrogen atoms are distributed over four positions with an occupation factor of 0.75, resulting in H$_3$O$^+$. The distance between the OH oxygen atom and O2 atom in the chain is 2.717 Å, so there is a medium strength hydrogen bond.

Oxonium salts of sulfates are already known in the literature. Kemnitz et al. described the alkali compounds A(H$_3$O)(HSO$_4$)$_2$ (A = Na,[12] K[13]) and oxonium hydrogensulfate, H$_3$O(HSO$_4$).[9] The oxonium cation in these compounds is also bonded to the anions by hydrogen bonds. In these compounds, the distances between donor and acceptor atoms are in the range 2.60 to 2.72 Å.

The B/S ratio of 1:2 was also found in Li[B(SO$_4$)$_2$] but this compound comprises a 3D net of corner-linked tetrahedra with a close similarity to modifications of SiO$_2$, especially to β-tridymite. With respect to the silicates, the borosulfate chain in H$_3$O[B(SO$_4$)$_2$] can be seen as analogous to the structure of SiS$_2$,[14] in which the SiS$_4$ tetrahedra are linked through common edges to a linear chain. Thus, the anionic network in H$_3$O[B(SO$_4$)$_2$] represents an "scaled-up" variant of SiS$_2$, or with regard to the H$_3$O$^+$ cation, it is a filled variant of CuFeS$_2$. To our knowledge, this motif is not known for silicates[15, 16] but was recently found for the borophosphate Na$_3$[B(PO$_4$)$_2$][17] and, in a more complex form, for MM'(H$_2$O)[B(PO$_4$)$_2$]·H$_2$O (M = Na, K; M' = Mg, Mn, Fe, Co, Ni, Zn).[18]

Generalised description: All crystal structures represent new structure types. Together with the recently described borosulfates A_5[(B(SO$_4$)$_4$] (A = Na, K), A_3[B(SO$_4$)$_3$] (A = K, Rb,), Li[B(SO$_4$)$_2$] and Li[B(S$_2$O$_7$)$_2$], a more general description and classification of these structures is possible. Because the structures of borosulfates (and borophosphates) are based on corner-sharing tetrahedra, the concept described by Liebau[15] is very useful for the systematic description. Kniep et al. modified and extended this concept for the description of borophosphates.[19] The extension was necessary because borophosphates consist of two different tetrahedra and boron can also show trigonal-planar coordination. As a result, the type of coordination is different for the boron polyhedra and fundamental building units were defined according to the geometry of the polyhedra themselves, the polyhedra's connection and the B/P ratio. In the case of borosulfates, the issue is simpler than for borophosphates for two reasons. First, boron was always found in BO$_4$ tetrahedra and has, thus far, never been found in a trigonal-planar unit in this class of compounds. Second, there are so far no examples of directly connected boron polyhedra.

The classification of all known borosulfates is shown in Table 1. The open-branched pentamer of [B(SO$_4$)$_4$]$^{5-}$ is only known for the alumosilicate Zunyite,[20] in which it is found not as a non-condensed moiety but incorporated into an AlO$_6$ octahedral network. This pentamer is also found in the borophosphates M_6[B(PO$_4$)$_4$][PO$_4$] (M = Pb, Sr).[21] A cyclo-branched or loop-branched pentamer [B(S$_2$O$_7$)$_2$]$^-$ is so far unknown in borophosphate chemistry. The open-branched vierer single chain [B(SO$_4$)$_3$]$^{3-}$ is, according to the isotypism, the same as in Ba$_3$[B(PO$_4$)$_3$].[22] The cyclo-branched vierer single chain in Cs[B(SO$_4$)(S$_2$O$_7$)] and H[B-(SO$_4$)(S$_2$O$_7$)], as well as the zwölfer framework in Li[B-(SO$_4$)$_2$], were observed for the first time. The loop-branched vierer single chain in H$_3$O[B(SO$_4$)$_2$] is the same as in Na$_3$[B-(PO$_4$)$_2$].[17]

Table 1. Classification of borosulfates according to Liebau[15] and Kniep et al.;[19] D = dimensionality, M = multiplicity, P = periodicity.

Compound	Connectivity	Branching	D	M	P
$K_5[B(SO_4)_4]$	$B^{4/4}, S^{1/4}$	open-branched pentamer	0	0	–
$Na_5[B(SO_4)_4]$-I					
$Na_5[B(SO_4)_4]$-II					
$Li[B(S_2O_7)_2]$	$B^{4/4}, S^{2/4}$	loop-branched or cyclo-branched pentamer	0	0	–
$Na[B(S_2O_7)_2]$					
$K[B(S_2O_7)_2]$					
$K_3[B(SO_4)_3]$]	$B^{4/4}, S^{1/4}, S^{2/4}$	open-branched vierer single chain	1	1	4
$Rb_3[B(SO_4)_3]$]					
$H[B(SO_4)(S_2O_7)]$	$B^{4/4}, S^{2/4}$	cyclo-branched vierer single chain	1	1	4
$Cs[B(SO_4)(S_2O_7)]$					
$Li[B(SO_4)_2]$	$B^{4/4}, S^{2/4}$	zwölfer framework	3	–	–
$H_3O[B(SO_4)_2]$	$B^{4/4}, S^{2/4}$	loop-branched vierer single chain	1	1	4

The deviations from the idealised tetrahedral structure can be quantified as described by Balic-Žunic and Makovicky.[23] Table 2 gives an overview of these deviations. Most of the deviations are less than 0.5 %, that is, the tetrahedra are quite regular. The variation resulting from the different

Table 2. Deviation from the ideal tetrahedral symmetry [%], as defined by Balic-Žunic and Makovicky.[23]

Compound	BO_4	SO_4	S_2O_7	BS_4
$K_5[B(SO_4)_4]$	0.43	0.08–0.23 (4×)		4.1
$Na_5[B(SO_4)_4]$-I	1.22/1.32	0.07–0.20 (8×)		14.6
$Na_5[B(SO_4)_4]$-II	0.46	0.10–0.35 (4×)		44.3/45.4
$H[B(SO_4)(S_2O_7)]$	0.15/0.32	0.40/0.53	0.11–0.20 (4×)	24.5/25.6
$Cs[B(SO_4)(S_2O_7)]$	0.38	0.31	0.14/0.17	26.2
$K_3[B(SO_4)_3]$]	0.58	0.11/0.55		3.1
$Rb_3[B(SO_4)_3]$]	0.65	0.14/0.76		2.8
$Li[B(S_2O_7)_2]$	0.26/0.98		0.07–0.28 (8×)	39.0/58.7
$Na[B(S_2O_7)_2]$	0.33		0.07–0.16 (4×)	45.0
$K[B(S_2O_7)_2]$	0.10/0.34		0.08–0.22 (8×)	36.9/45.3
$H_3O[B(SO_4)_2]$	0.31	0.26		5.0
$Li[B(SO_4)_2]$	0.19/0.33	0.13–0.55 (8×)		1.5/2.4

connection modes (splitting of distances to O^{term}, O^{br} and $O^{H\,bond}$, and of angles O-B-O and O-S-O) have already been discussed. The general tendency is that deviations in the BO_4 tetrahedra are larger than in the SO_4 tetrahedra, and disulfate groups are more regular than isolated sulphate ions, both presumably due to the higher formal charges of the central ions involved.

All borosulfates that are known to date show BO_4 tetrahedra surrounded by SO_4 tetrahedra. Therefore, BS_4 "supertetrahedra" (i.e., "tetrahedra of tetrahedra") can be defined and their deviation from idealised symmetry can be calculated (Table 2). The values show that large deviations occur for all compounds containing $S_2O_7^{2-}$ units. Surprisingly, the deviations are below 5 % for all compounds with SO_4^{2-} ions, except $Na_5[B(SO_4)_4]$, in which significant differences are present for the two forms of $Na_5[B(SO_4)_4]$. The small deviations for the SO_4-based compounds again show the topological relationship between borosulfates and silicates.

Conclusion

A visual review of the known structural motifs of borosulfates is shown in Figure 16. Because six different types are now characterised, some first general tendencies can be derived. To date, we have not observed compounds with boron
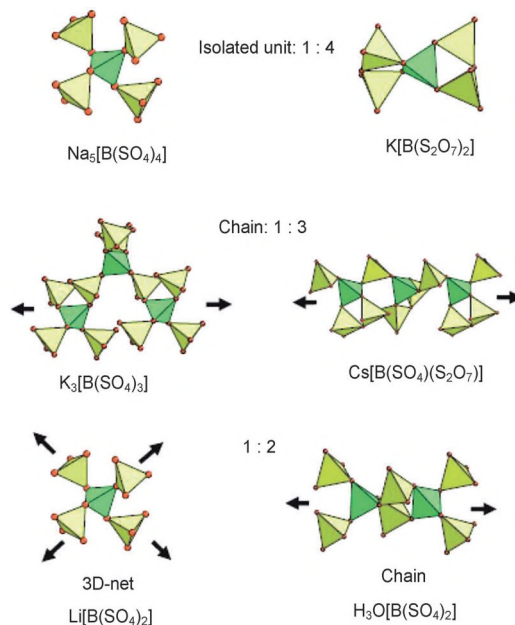

Figure 16. Building units in borosulfates.

in a trigonal-planar coordination mode, in contrast to borates and borophosphates. This might be explained by the significantly lower-charged oxygen atoms from the sulfate groups—four oxygen atoms from four sulfate groups deliver significantly less negative charge than if they were bound to phosphate or borate moieties, thus avoiding an overload for the central boron atom. Furthermore, there are no examples of directly connected boron tetrahedra, which is also different to borophosphates. On the other hand, and very surprisingly, we have already found several examples of directly condensed SO_4 tetrahedra, that is, disulfate anions as ligands. Therefore, the modified "Loewenstein rule,"[24] commonly used to explain the prevention of the formation of Al-O-Al units in alumosilicates, is valid in borosulfates, only for B-O-B and not S-O-S units. This is really astonishing since the Loewenstein rule deals with charge repulsion, which should be significantly larger in neighbouring sulfate tetrahedra than for borate tetrahedra. This is the opposite of borophosphates, for which B-O-B situations occur but not P-O-P.

Our new borosulfates are examples of the realisation of different structural characteristics by an exchange of SO_4 and S_2O_7 groups. This leads to new connectivity modes and changes the charge of the complex anions, despite the B/S ratio being the same. Examples are the pairs $A_5[B(SO_4)_4]$/$A[B(S_2O_7)_2]$ and $A_3[B(SO_4)_3]$/$A[B(SO_4)(S_2O_7)]$. A new field

may be opened by the introduction of other oligosulfates, although very few are known ((NO_2)$_2$[S_3O_{10}],[25] (NO_2)$_2$-[S_4O_{13}],[26] $K_2S_5O_{16}$[27]). Recent work by Wickleder et al. has shown that longer chain fragments, [(SO_3)$_n$$SO_4$]$^{2-}$, can act as ligands ($n=2$: Pb($S_3O_{10}$);[28] $n=3$: $K_2Pd(S_4O_{13})_2$)[29]).

Finally, there might be further compounds of unusual cations like the oxonium ion, H_3O^+, which are not yet known for silicates but are well-known for borophosphates.[19] Another remarkable feature is the existence of a polyacid, H[B(SO_4)(S_2O_7)], which is also not (yet) paralleled in borophosphates. Both aspects are probably caused by the fact that oleum is a very acid solvent.

We are still at the beginning of the exploration of borosulfates as a new, exciting class of compounds. As this contribution shows, their compositions and crystal structures will confirm some expectations coming from silicates and borophosphates but will also offer some surprises.

Experimental Section

Syntheses:

Na[B(S_2O_7)$_2$]: The synthesis was performed at room temperature by starting from sodium sulfate hydrate, boron oxide and oleum. A mixture of sodium hydrogensulfate hydrate (NaHSO$_4$·H$_2$O, 1.510 g, 11 mmol, Grüssing, 99%) and boron oxide (B$_2$O$_3$, 0.947 g, 13.5 mmol, ABCR, 99.6%) was charged with oleum (10 mL, Merck, 65% SO$_3$). After one week the precipitate was collected in the absence of air.

K[B(S_2O_7)$_2$]: K$_2$S$_2$O$_7$ (3.9 g, 15.5 mmol, Merck, p.a.) and B$_2$O$_3$ (1.0 g, 14.3 mmol, ABCR, 99.6%) were added to oleum (10 mL, Merck, 65% SO$_3$). After one week the precipitate was collected.

Cs[B(SO$_4$)(S_2O_7)]: Caesium chloride (1.728 g, 10 mmol, Aldrich, 99.9%) and boron oxide (0.996 mg, 14 mmol, ABCR, 99.6%) were dissolved in H$_2$SO$_4$ (6 mL, Fa. Merck, conc., 96%). When the formation of HCl had completely finished, oleum (10 mL, Merck, 65% SO$_3$) was added. After one week, colourless, moisture-sensitive crystals were formed. The precipitate was collected.

H[B(SO$_4$)(S_2O_7)]: Oleum (20 mL, Merck, 65% SO$_3$) was added to B$_2$O$_3$ (10 g, 0.14 mol, ABCR, 99.6%) in a Schlenck tube. When the release of SO$_3$ gas was finished, the Schlenck tube was closed. After several days, colourless platelets were formed on the surface of the liquid. The crystals were easily broken into thin rods on application of mechanical stress.

H$_3$O[B(SO$_4$)$_2$]: B$_2$O$_3$ (210 mg, 3.0 mmol, ABCR, 99.6%) and oleum (0.75 mL, Merck, 65% SO$_3$) were placed in an silica glass ampoule (volume 2 mL, length 4 cm), enclosed in an autoclave, heated to 100°C for 5 d and cooled to RT at a rate of 6 K h^{-1}.

Crystallised products: All crystals were colourless. According to their morphology, single-phase products can be assumed. For each compound, several crystals were tested, leading to the same unit cell. Except H$_3$O[B(SO$_4$)$_2$], all crystals started to decompose more or less rapidly, when they were separated from the mother liquor. For H$_3$O[B(SO$_4$)$_2$], an XRD pattern was recorded showing the expected lines of H$_3$O[B(SO$_4$)$_2$] with some additional lines of an unknown compound.

Crystal-structure determination: All crystal structures were determined and refined with single-crystal data. Crystals were directly prepared from the mother-liquor solutions. Room temperature data were measured with an Image Plate Diffraction System (IPDS II, Stoe) with Mo$_{K\alpha}$ radiation. Low-temperature data (at 150 K) were recorded with a Nonius-D8 diffractometer with an APEX II detector and a micro-source (Mo radiation). Structure solution by Direct Methods and refinement were performed with SHELXTL.[30] Data acquisition, generation of a data set, cell refinement, and absorption correction were performed by using software provided by the diffractometer supplier.[31,32] Further details of the

crystal structure investigations can be obtained from the Fachinformationszentrum Karlsruhe, 76344 Eggenstein-Leopoldshafen, Germany (fax: (+49) 7247-808-666; e-mail: crysdata@fiz-karlsruhe.de, http:// www.fiz-karlsruhe.de/request_for_deposited_data.html) on quoting the depository numbers CSD-426424 (Na[B(S_2O_7)$_2$]), CSD-426423 (K[B-(S_2O_7)$_2$]), CSD-426420 (Cs[B(SO$_4$)(S_2O_7)], CSD-426422 (H[B(SO$_4$)-(S_2O_7)]), and CSD-426421 (H$_3$O[B(SO$_4$)$_2$]).

Na[B(S_2O_7)$_2$]: Space group $P2_1/c$; $a=10.9489(2)$, $b=8.5491(2)$, $c=12.7013(3)$ Å; $\beta=110.227(1)°$; $Z=4$; 150 K; $2\theta_{max}=70°$; 22185 reflections measured; 4940 independent reflections; 3632 with $I>2\sigma(I)$; 182 parameters; $R_1(F)=0.037$, $wR_2(I)=0.083$.

K[B(S_2O_7)$_2$]: Space group Cc; $a=11.3368(1)$, $b=814.6662(2)$, $c=13.6650(1)$ Å; $\beta=94.235(1)°$; $Z=8$; 150 K; $2\theta_{max}=80°$; 49073 reflections measured; 12169 independent reflections; 11953 with $I>2\sigma(I)$; 361 parameters; $R_1(F)=0.015$; $wR_2(I)=0.042$.

Cs[B(SO$_4$)(S_2O_7)]: Space group $P2_1/c$; $a=10.4525(2)$, $b=11.3191(2)$, $c=8.2760(1)$ Å; $\beta=103.206(1)°$; $Z=4$; 150 K; $2\theta_{max}=70°$; 28818 reflections measured; 4184 independent reflections; 3906 with $I>2\sigma(I)$; 145 parameters; $R_1(F)=0.014$; $wR_2(I)=0.036$.

H[B(SO$_4$)(S_2O_7)]: Space group $P2_1/c$; $a=15.6974(10)$, $b=11.4362(7)$, $c=8.5557(6)$ Å; $\beta=90.334(3)°$; $Z=8$; 150 K; $2\theta_{max}=55°$; 20095 reflections measured; 3503 independent reflections; 3308 with $I>2\sigma(I)$; 281 parameters; $R_1(F)=0.032$, $wR_2(I)=0.081$; refined as a pseudo-merohedral twin, H atom fixed.

H$_3$O[B(SO$_4$)$_2$]: Space group $P4/ncc$; $a=9.1377(13)$, $c=7.3423(15)$ Å; $Z=4$; 293 K; $2\theta_{max}=58°$; 1376 reflections measured; 417 independent reflections; 294 with $I>2\sigma(I)$; 35 parameters; $R_1(F)=0.030$; $wR_2(I)=0.059$; H atom fixed with site occupation factor 0.75.

[1] H. A. Höppe, K. Kazmierczak, M. Daub, K. Förg, F. Fuchs, H. Hillebrecht, *Angew. Chem.* **2012**, *124*, 6359–6362; *Angew. Chem. Int. Ed.* **2012**, *51*, 6255–6257.

[2] M. Daub, K. Kazmierczak, P. Gross, H. Höppe, H. Hillebrecht, *Inorg. Chem.* **2013**, *52*, 6011–6020.

[3] C. Logemann, M. S. Wickleder, *Inorg. Chem.* **2011**, *50*, 11111–11116.

[4] ##. Bruns, M. Eul, R. Pöttgen, M. S. Wickleder, *Angew. Chem.* **2012**, *124*, 2247–2250; *Angew. Chem. Int. Ed.* **2012**, *51*, 2204–2207.

[5] C. Logemann, T. Klüner, M. S. Wickleder, *Chem. Eur. J.* **2011**, *17*, 758–760; C. Logemann, K. Rieß, M. S. Wickleder, *Chem. Asian J.* **2012**, *7*, 2912–2920.

[6] K. Ojima, Y. Nishihata, A. Sawada, *Acta Crystallogr. Sect. A Acta Crystallogr. B* **1995**, *51*, 287–293.

[7] T. Steiner, *Angew. Chem.* **2002**, *114*, 50–80; *Angew. Chem. Int. Ed.* **2002**, *41*, 48–76.

[8] Reflections violating a *C* centring are significantly weaker ($I/(\sigma)I=13$) than the reflections from the complete data set ($I/(\sigma)I=26$).

[9] E. Kemnitz, C. Werner, S. Trojanov, *Acta Cryst. C* **1996**, *52*, 2665–2668.

[10] W. Hönle, *Z. Kristallogr.* **1991**, *196*, 279–288.

[11] M. O'Keeffe, *Acta Cryst. Sect. A* **1977**, *33*, 914–923.

[12] a) S. Trojanov, C. Werner, E. Kemnitz, H. Worzala, *Z. Anorg. Allg. Chem.* **1995**, *621*, 1617–1624.

[13] E. Kemnitz, C. Werner, S. Trojanov, H. Worzala, *Z. Anorg. Allg. Chem.* **1994**, *620*, 1921–1924.

[14] J. Peters, B. Krebs, *Acta Crystallogr. Sect. A Acta Crystallogr. B* **1982**, *38*, 1270–1272.

[15] F. Liebau, *Structural Chemistry of Silicates*, Springer, Heidelberg, **1985**.

[16] P. Villars, L. D. Calvert, *Pearson's Handbook, Crystallographic Data for Intermetallic Phases*, ASM International, Materials Park, OH, **1997**; CD-ROM version **2011**.

[17] D.-B. Xiong, H.-H. Chen, X.-X. Yang, J.-T. Zhao, *J. Solid State Chem.* **2007**, *180*, 233–239.

[18] R. Kniep, H. G. Will, I. Boy, C. Röhr, *Angew. Chem.* **1997**, *109*, 1052–1054; *Angew. Chem. Int. Ed. Engl.* **1997**, *36*, 1013–1014.

[19] a) R. Kniep, H. Engelhard, C. Hauf, *Chem. Mater.* **1998**, *10*, 2930–2934, und b) B. Ewald, Y.-X. Huang, R. Kniep, *Z. Anorg. Allg. Chem.* **2007**, *633*, 1517–1540.

[20] L. Pauling, *Z. Kristallogr.* **1933**, *84*, 442–452; W. H. Baur, T. Ohta, *Acta Cryst. B* **1982**, *38*, 390–401.

[21] E. L. Belokoneva, E. A. Ruchkina, O. V. Dimitrova, S. Yu. Stefanovich, *Russ. J. Inorg. Chem.* **2001**, *46*, 179–185. N. Shiu, J. Kim, D. Ahn, K.-S. Sohn, *Acta Cryst. C* **2005**, *61*, i54–56.

[22] R. Kniep, G. Gözel, B. Eisenmann, C. Röhr, N. Asbrand, M. Kizilyalli, *Angew. Chem.* **1994**, *106*, 791–793; *Angew. Chem. Int. Ed. Engl.* **1994**, *33*, 749–751.

[23] T. Balic-Žunic, E. Makovicky, *Acta Cryst. B* **1996**, *52*, 78–81. E. Makovicky, T. Balic-Žunic, *Acta Cryst. Sect. B* **1998**, *54*, 766–773.

[24] W. Loewenstein, *Am. Mineral.* **1954**, *39*, 92–96.

[25] a) J. W. Steeman, C. H. MacGillavry, *Acta Cryst.* **1954**, *7*, 402–404; b) K. Eriks, C. H. MAcGillavry, *Acta Cryst.* **1954**, *7*, 430–434; c) D. W. J. Cruickshank, *Acta Cryst.* **1964**, *17*, 684–685.

[26] C. Logemann, T. Klüner, M. S. Wickleder, *Angew. Chem.* **2012**, *124*, 5082–5085; *Angew. Chem. Int. Ed.* **2012**, *51*, 4997–5000.

[27] R. De Vries, F. C. Mijlhoff, *Acta Cryst. B* **1969**, *25*, 1696–1699.

[28] C. Logemann, T. Klüner, M. S. Wickleder, *Z. Anorg. Allg. Chem.* **2012**, *638*, 758–762.

[29] J. Bruns, T. Klüner, M. S. Wickleder, *Angew. Chem.* **2013**, *125*, 2650–2652; *Angew. Chem. Int. Ed.* **2013**, *52*, 2590–2592.

[30] G. M. Sheldrick, *SHELXTL* program package, University of Göttingen, Germany, **1997**.

[31] *Program XAREA,* XSHAPE, XRED, Stoe Cie. Darmstadt, Germany.

[32] a) T. Remove, *SAINT,* Data reduction and frame integration program for the CCD area-detector system, Bruker Analytical X-ray Systems, Madison, Wisconsin, USA, **2006**; b) G. M. Sheldrick, *SADABS*, Program for area detector adsorption correction, Institute for Inorganic Chemistry, University of Göttingen, Germany, **1996**.